RESISTIVE BALLOONING MODES UNDER PLASMA EDGE CONDITIONS

K. Grassie and H.P. Zehrfeld

Max-Planck-Institut für Plasmaphysik
EURATOM Association, D-8046 Garching, Federal Republic of Germany

C.M. Bishop, R.J. Hastie and T.C. Hender

Culham Laboratory
UKAEA / EURATOM Fusion Association
EURATOM Association, Abingdon, Oxfordshire, OX14 3 DB, U.K.

Introduction: Recently resistive ballooning modes have become the object of intensified theoretical investigation. The reason for this increased interest is that they may be linked to confinement degradation observed in tokamak experiments at high plasma pressure. In previous publications [1,2] we investigated the ballooning stability of ASDEX high-β_p discharges and demonstrated that the hard β_p-saturation observed in ASDEX can be naturally explained within the framework of resistive ballooning modes. Here we concentrate the investigation to the region near the separatrix. Furthermore we include a detailed discussion of resistivity effects on the second stable regime. This analysis is based on an analytic large aspect-ratio model for plasma equilibrium in the neighbourhood of a given flux surface (local equilibrium) [3]. Finally, we comment on the resistive stability of toroidal 2-D ASDEX equilibria with experimentally determined current and pressure profiles.

Local equilibria and second region of resistive ballooning stability: To elucidate the characteristic features of the problem in terms of a limited number of parameters we refer to the theory of a local equilibrium presented in [3]. The shape of the flux surfaces is controlled by assigning particular values to the expression

$$(1) \quad k^2 = r^2(\sqrt{(1+k)}-1)^2[4 + r^2(\sqrt{(1+k)}-1)^2 - 4r\cos(\theta-\theta_x)(\sqrt{(1+k)}-1)].$$

Here (r,θ) are polar coordinates with the radius r normalized by a geometrical parameter r_0. θ_x is the angular position of the X-point and k the distortion of the flux surface; $k=1$ is the separatrix case and $k=0$ is a circle. The resulting resistive ballooning equations are

$$(2) \qquad \frac{b}{h}\frac{d}{d\theta}[\frac{b}{hL}(\frac{1}{b^2}+P^2)\frac{du}{d\theta}] - \alpha K(u+v) - \gamma^2(\frac{1}{b^2}+P^2)u = 0$$

and

$$(3) \quad \frac{b}{q^2h}\frac{d}{d\theta}[\frac{b}{h}\frac{dv}{d\theta}] + \alpha K[4\frac{\gamma^2}{\alpha^2} + \frac{\eta n^2}{S_A\gamma}]u - \{\frac{\eta n^2}{S_A\gamma}[-\alpha K + \gamma^2(\frac{1}{b^2}+P^2)] + \frac{\gamma^2}{q^2}\frac{1+\beta}{\beta}\}v = 0$$

where W, D, b, h and f are defined in [5] and

$$K = -\frac{1}{h}[P(\frac{dr}{d\theta}cos\theta - rsin\theta) + \frac{1}{b}(\frac{dr}{d\theta}sin\theta - rcos\theta)]$$

$$P = -b\int [\alpha\frac{W}{D} - \Lambda + 2\frac{b}{f} - \alpha rcos\theta]\frac{h}{b^3}d\theta$$

$$L = 1 + \frac{\eta n^2}{S_A\gamma}[\frac{1}{b^2} + P^2],$$

with $\alpha = -2\mu_0 r_0 r^2 p'/B_p{}^2$, $\beta = \gamma_T\mu_0 p/B^2$, the magnetic Reynolds number $S_A = \tau_R/\tau_A$ and the ratio of the specific heats $\gamma_T = c_p/c_V$ and the growth rate γ is normalized to the Alfvén frequency $\gamma_A = \sqrt{r_0{}^2 B_p{}^2/(r^2\mu_0\rho)}$

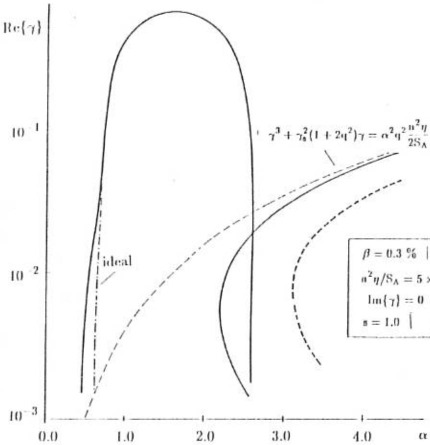

Fig.1

In the limit of circular flux surfaces ($k = 0$) these equations reduce to the $s - \alpha$ model, with the shear s related to the current density parameter Λ by $s = 2 - \Lambda$. We start the investigation of the second regime in this limit. Fig.1 shows the real part of the growth rate versus α for ideal ballooning modes (dot-dashed line) and resistive modes (solid lines). The hat-shaped curve shows second stability behaviour. The slight bulge in this curve at $\alpha \sim 0.6$ indicates the transition to overstability [6]. This resistive curve closely parallels the ideal stability curve and is reproduced by the Δ'-criterion for resistive ballooning modes [6,7] to reasonable accuracy:

(4)
$$\Delta' = \frac{2\gamma^{5/4}(1+2q^2)^{1/4}}{S_A(\eta^2 s^2 q^2/S_A)^{3/4}}\left\{\frac{\Gamma(\frac{1}{4})}{\Gamma(\frac{3}{4})} - \frac{\Gamma(\frac{1}{4}+\frac{\hat{\gamma}}{4})}{\Gamma(\frac{3}{4}+\frac{\hat{\gamma}}{4})}\right\}^{-1}.$$

with $\hat{\gamma} = \gamma\gamma_A/\gamma_R$, $(\gamma_R/\gamma_A)^3 = n^2\eta s^2 q^2\beta^2(1+2q^2)/S_A$ and where Δ' is in general to be evaluated numerically [8]. This dispersion relation (4) is derived in the limit $\gamma << \gamma_S = \sqrt{\beta}$, where γ_S denotes the sound frequency. In the other limit ($\gamma >> \gamma_S$) a compressibility mode, not driven by Δ', can occur. Its growth rate is governed by the dispersion relation [9]

(5)
$$\gamma^3 + \gamma_S{}^2(1+2q^2)\gamma = \alpha^2\frac{\eta n^2 q^2}{2S_A}$$

This mode can also be seen to occur in our numerical results in Fig.1, where the branch occuring for $\alpha > 2.6$ ($\beta = 3 \times 10^{-3}$) is compared with the solution of (5) (long-dashed line). It should be noted that in general $\gamma << \gamma_S$ for typical tokamak parameters, but in the second stable regime the high α-values make the region where $\gamma \sim \gamma_S$ more accessible. From Fig.1 it can be seen that the dispersion relation (5) continues to apply reasonably well to the regime $\gamma > \gamma_S$ where $\gamma \propto \eta/(S_A {\gamma_S}^2)$. Thus we conclude that the existence of a second stable regime depends on γ_S and S_A – for large enough values of either parameter a second stable region exists below the critical value of α at which compressibility modes (5) are destabilized. This is separately demonstrated by the short dashed curve in Fig.1, representing the compressibility mode for $\beta = 5 \times 10^{-3}$. The corresponding hat-shaped solutions are essentially unchanged with respect to this increase in β, so that effectively a second stable window exists for this case. It should be noted that the picture is in general more complicated, since the region of instability has to be maximized by optimizing the free parameter θ_0 which appears in eqs.3,4. Our conclusions presented above, however, are not affected by the variation of θ_0. Furthermore we find similar results on the basis of a model where the Shafranov shift of circular flux surfaces is taken into account.

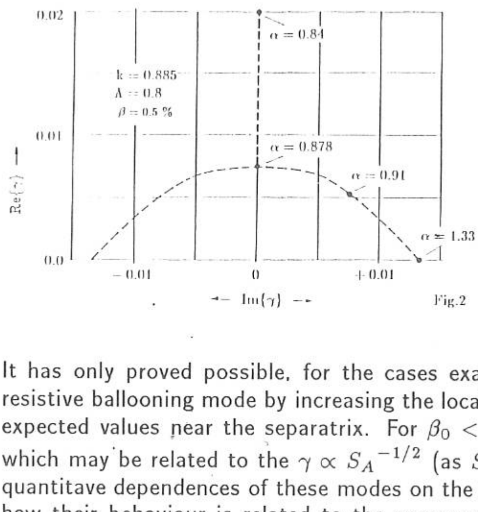

Fig.2

We now move on to study the non-circular case, i.e. $k > 0$. Fig.2 shows for $k = 0.885, \Lambda = 0.8$ the growth rate in the complex γ-plane for a branch entering a second stable resistive ballooning regime. There are, however, branches with $\gamma > \gamma_S$ which do not show second regime stability as α is increased; these branches can be supressed by increasing the sound frequency.
For the ideal ballooning mode coalescence of the first and second stable regime occurs as the separatrix is approached ($k \to 1$) for a sufficiently high current density parameter [5].
It has only proved possible, for the cases examined, to obtain this coalescence for the resistive ballooning mode by increasing the local β_0 to 5%, which is rather larger than the expected values near the separatrix. For $\beta_0 < 5\%$ and large $k > 0.9$ an unstable mode, which may be related to the $\gamma \propto {S_A}^{-1/2}$ (as $S_A \to \infty$) branches of Ref.10, occurs. The quantitave dependences of these modes on the parameter k and the question whether and how their behaviour is related to the appearence of compressibility modes is still under investigation.

<u>Ballooning stability in the ASDEX separatrix region:</u> We now briefly examine the ballooning stability of a typical ASDEX high-β_p discharge by solving the full resistive ballooning equations on the basis of a separatrix-bounded MHD equilibrium [1,2]. To make parametric studies we alter the value of the pressure gradient from the experimentally observed quantity using a multiplication factor C_p. Results for the real part of the growth rate versus this factor C_p are shown in Fig.3 for various flux surfaces from $r/a \simeq 0.87$ to $r/a \simeq 0.994$.

In line with our previous results [1,2] we find a transition from purely growing to overstable modes, when compressibility effects become important.

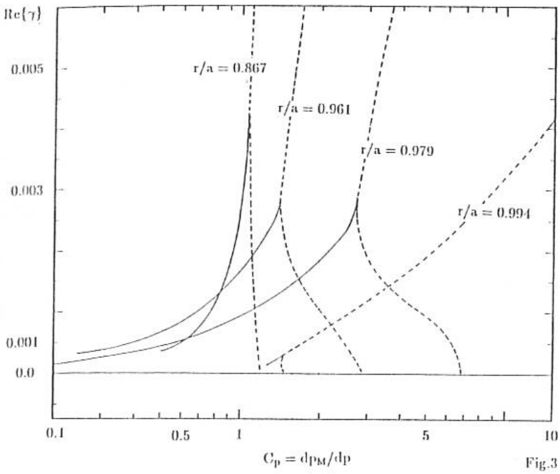

Fig.3

As soon as the bifurcation into the complex γ-plane occurs, the real solutions form separate branches which move to larger multiplication factors with decreasing growth rates (dashed lines), whereas the overstable branches (solid lines) show the opposite behaviour and are therefore the more unstable solutions.

From the observation that the bifurcation to overstability moves to smaller values of $Re\{\gamma\}$ when r/a increases ($\rightarrow \eta$ decreases and the strong compressibility dependence of the bifurcation point we conclude that the overstable branches are associated with the propagation of ion sound waves [6].

Interpreting these results in terms of absolute pressure gradients we find that the higher-shear surfaces close to the separatrix can support larger pressure gradients.

Conclusions: To summarize we have found that in the separatrix region resistive ballooning modes are generally more stable than in the plasma confinement region. However, we have demonstrated that for a second resistive ballooning stable regime to exist sufficiently large values for γ_S or S_A are required. Ideal calculations for the local separatrix equilibrium model show Bishop's results [4,5] for coalescence of the first and second stable regimes as the separatarix is approached ($k \rightarrow 1$). In the resistive case we find that separatrix effects are only strong enough to completely stabilize a ballooning mode at rather large values of $\beta_0 (> 5\%)$. Consequently the coalescence effect is restricted to this region of parameter space. Whether the small growth rates, which in general accompany resistive ballooning modes near $k = 1$, inhibit the L-H transition predicted in Refs. 4,5, requires additional analysis. Finally we found ASDEX high-β_p equilibria to be resistively unstable with small growth rates below the maximum value of β_p. In the separatrix region larger absolute pressure gradients are supported so that growth rates decrease and corresponding effects on the transport do not appear to be significant here.

1. K. Grassie and H.P. Zehrfeld, IPP Report 5/16 (1987) (to be published in Nucl. Fus.).
2. K. Grassie and H.P. Zehrfeld, Signatures of Resistive Ballooning Modes For ASDEX High Beta Discharges (1987) (to be published in Nucl. Fus.).
3. C.M. Bishop, Culham Report CLM-R249.
4. C.M. Bishop, Nucl. Fusion **24**, p. 1579.
5. C.M. Bishop, Nucl. Fusion **26**, p. 1063.
6. J.W Connor et. al., Baltimore IAEA **III**, p. 403.
7. J.F Drake and T.M. Antonsen, Phys. Fluids **28**, p. 544.
8. A. Sykes et. al., Plasma Physics **29**, p. 719.
9. T.C. Hender et. al., Phys. Fluids **27**, p. 1439.
10. A.H. Glasser et. al., Proc. Oxford EPS, paper A 3.1.